Periodic Resonance Excitation and Intertube Interaction from Quasicontinuous Distributed Helicities in Single-Wall Carbon Nanotubes

M. Milnera,[1] J. Kürti,[2] M. Hulman,[1] and H. Kuzmany[1]
[1]*Universität Wien, Institut für Materialphysik, Strudlhofgasse 4, A-1090 Wien, Austria*
[2]*Eötvös University, Department of Biological Physics, H-1117 Budapest, Hungary*
(Received 16 August 1999)

Photoselective resonance Raman scattering from laser ablation grown single-wall carbon nanotubes is demonstrated to be consistent with a response from tubes with all geometrically allowed helicities. This information is drawn from an analysis of the resonance scattering by combining *ab initio* calculations for the mode frequencies with evaluations of the resonance cross sections for isolated tubes. The resonance excitation was found to exhibit an oscillatory behavior. To match the experiments and the calculations, the frequencies obtained from the latter must be up-shifted by 8.5% on the average. This stiffening is ascribed to the tube-tube interaction in the carbon nanotube bundles.

PACS numbers: 78.30.–j, 63.20.Dj, 78.66.Qn

Single-wall carbon nanotubes (SWCNTs) have an extended spectrum of interesting physical properties. This spectrum is not yet fully explored but it covers, among others, unusual mechanical properties, quantum-size effects in the electronic properties, photoselective resonance scattering in Raman experiments, and attractive catalytic and electrochemical behavior. Some of these properties have been analyzed in single-tube experiments where details of the geometric structure of the tubes can be determined. In general, this is not possible and tubes with different diameters and different helicities are packed into bundles and contribute as such to the experimental response. In the early days of research work on SWCNTs, a dominance of (10,10) armchair tubes was anticipated [1,2] but Raman scattering always revealed a rather large number of peaks for the radial breathing mode (RBM) which was difficult to understand from scattering of predominantly (10,10) tubes. In addition recently scanning tunneling microscopy [3], high resolution electron microscopy [4], and detailed Raman analyses of the RBM [5,6] demonstrated that many more helicities with different diameters are dispersed in the samples. Theoretical evaluations of ground state energies of the tubes did thus far not come up with any preferred tube geometry so that, even for a rather narrow range of diameters, as determined, e.g., from electron microscopy, a continuous distribution of tubes among the helicities must be expected. For the classical tube material as it was described in Ref. [1], the diameter distribution allows for more than 60 different tubes if all geometrically possible helicities are included. Under these conditions it remained a puzzle why the Raman response of the RBM is still dominated by a well-expressed fine structure as it would be expected for a discrete set of helicities for the tubes.

The crucial role of the RBM for the analysis of SWCNTs originates from the fact that its frequency scales with the inverse of the tube diameter D. This leads eventually, together with the similar scaling of the electronic transition energies, to a well-expressed photoselective resonance scattering in Raman experiments. Both effects, the scaling with $1/D$ and the photoselective resonance scattering, have been reported in several papers [7–10] and the line shape of the RBM was repeatedly reported to exhibit a fine structure. However, for a quasicontinuous distribution of diameters a smearing out of all fine structure is expected.

In this Letter we demonstrate the following: (i) The observed structures in the optical absorption and the fine structure in the Raman response for the RBM are in detail consistent with contributions from all geometrically allowed tubes in a certain diameter range. (ii) The Raman response of the RBM exhibits an oscillatory behavior with respect to the excitation energy. This oscillation refers to the frequency at maximum intensity and to the maximum intensity itself and is a result of the superimposed resonance scattering from the Van Hove singularities of the various tubes. (iii) The fine structure of the Raman response is at least semiquantitatively retained from *ab initio* calculations on isolated tubes, combined with an evaluation of the resonance cross section. (iv) The absolute values for the evaluated peak positions must be up scaled on the average by 8.5% to match the experiments which is considered as a quantitative evidence for the strong interaction of the individual tubes in the bundle.

The SWCNTs used in this work were grown from a two beam laser desorption process described previously [1]. According to the original analysis and many later works on related materials, the average diameter of the tubes is around 1.38 nm which corresponds to a (10,10) armchair species. Slightly lower values were reported from electron microscopy. For the optical transmission experiments, thin films were prepared by peeling the tubes from a microporous filter with a scotch tape after they had been suspended and filtered from a solution of alcohol with a surfactant.

For the Raman excitation, a large number of different lasers were used, extending from the deep blue (2.7 eV)

 0031-9007/00/84(6)/1324(4)$15.00

to the infrared (1.16 eV). Since any purification process was observed to result in a smearing out of fine structure in the Raman response due to a broadening of the individual peaks, the tubes were measured as prepared from the laser ablation. Raman excitation was performed in high vacuum with the excitation power kept below 1 mW to avoid heating by the laser beam. Analysis was performed with a Dilor xy system as described previously [5]. The response of the spectrometer was calibrated using the resonance behavior of the F_{1g} mode of Si [11].

The number of different laser lines used to record the Raman response in the spectral range of the RBM was large enough to follow the rather rapid but still continuous development of the spectra at least in part of the energy range under investigation. This change of the spectra with excitation energy is so fast that Stokes and anti-Stokes recorded spectra or any weak heating of the sample by the laser resulted in a different line shape as a consequence of the different electronic and vibronic states involved. Selected recorded spectra are presented in Fig. 1(a). Except for the multipliers indicated, the intensities of the spectra are comparable. There is a well-expressed fine structure in the spectra as it has been observed previously several times. The change of this fine structure appears rather chaotic at a first glance. However, watching in detail reveals that the intensities and line positions change periodically with the laser energy. There are at least two transitions to very low intensity around 800 nm and around 600 nm. Each time the transition to low intensity is passed the peak position of the response switches to a lower value. To better characterize this oscillatory behavior, the positions of the peaks are plotted versus the excitation energy in Fig. 2. The value of the periodicity is approximately 0.6 eV.

As stressed above there is no good reason to make a selected group of tubes responsible for this particular behavior. We thus evaluated the response from all tubes in the relevant diameter range. Since the observed peaks in the spectra extended from about 145 to 220 cm^{-1}, 80 different geometrically allowed tubes must be considered. The joint density of states (JDOS) for all these tubes was evaluated using the zone folding technique. To save computer time the dispersion relations for the chiral tubes was expanded in a Taylor series up to quadratic order in k. The resulting JDOS exhibited the typical Van Hove singularities for all chiralities. For the comparison with the experiments the $pp\pi$ matrix element γ_0 was varied between 2.5 and 3.1 eV. A value of 2.9 eV was found to yield best agreement.

Relevant for the resonance Raman scattering are the first and second resonance transitions in the case of the metallic tubes and the second, third, and fourth resonance transition in the case of the semiconducting tubes. Whereas the low energy transitions exhibit the well-known uniform scaling with the diameter [12], this is not so for the higher transition. As a consequence the superposition of all contributions to the overall JDOS smears out for almost the whole energy range and eventually the JDOS of the graphene sheet is obtained. This is demonstrated in Fig. 3(a) where the superposition of the 80 JDOS was weighted with a Gaussian distribution of the diameters with a mean value and a variance of $D = 1.35$ nm and $\sigma^2 = 0.01$ nm^2, respectively. Only for the low energy part of the superposition a structure is retained. This is demonstrated in Fig. 3(b). Under the well-justified assumption that the resonances between Van Hove singularities in the density of states dominate the JDOS and thus the optical absorption, the resulting pattern can be compared directly with the optical transmission of a thin film. As demonstrated in the figure this comparison is very satisfactory for energies including the whole visible spectral range.

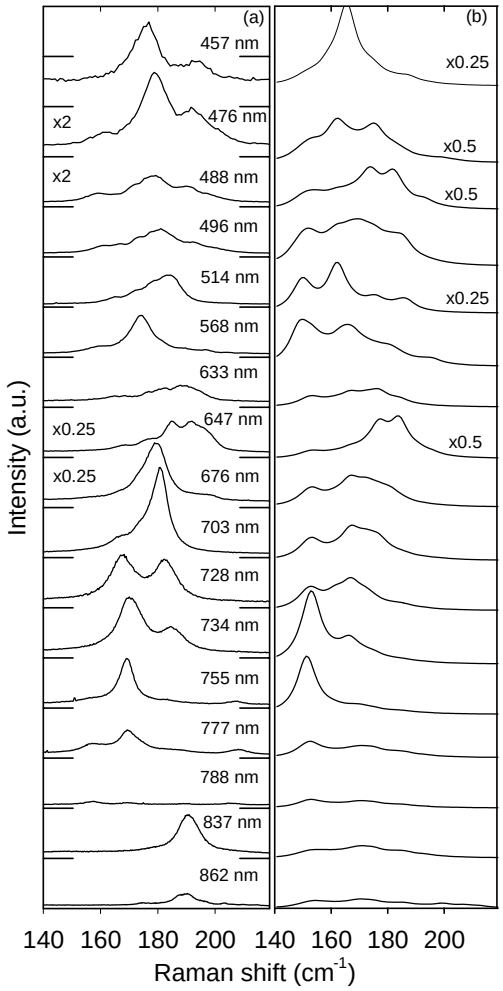

FIG. 1. Raman response for the radial breathing mode of single-wall carbon nanotubes as excited with different lasers (a) and calculated response for 80 different tubes (b). Relative intensities in (a) are calibrated from the resonance of the F_{1g} mode in Si. Scaling factors are multipliers for the as-measured (calculated) spectra.

For the evaluation of the Raman response we proceed similarly. The RBM frequencies for the armchair and zigzag tubes were calculated using the Vienna

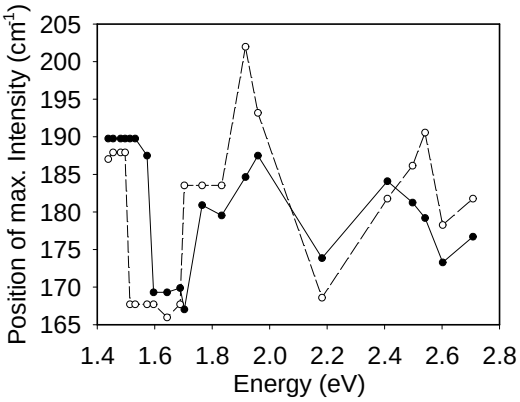

FIG. 2. Peak position of the radial breathing mode for excitation with various lasers: (•, —) as measured; (∘, – – –) as calculated with an 8.5% up-shift in frequency.

ab initio simulation package (VASP) as reported previously [13]. From these results the frequencies for the chiral tubes were determined by interpolation from $\nu = [239 - 5(n - m)/n]/D(n, m)$. The average distance between frequencies is less than 1 cm^{-1} but the evaluated frequencies are slightly clustered. The result still confirms the quasicontinuous distribution of the modes. Each frequency was broadened with a Lorentzian line of width 4 cm^{-1} and the peak intensity I_0 was evaluated from the JDOS $g(\epsilon)$ according to [14]

$$I_0 = \left| \int \frac{g(\epsilon) d\epsilon}{(\hbar\omega_{\mathrm{i}} - \epsilon - \mathrm{i}\hbar\alpha)(\hbar\omega_{\mathrm{s}} - \epsilon - \mathrm{i}\hbar\alpha)} \right|^2 . \quad (1)$$

The above relation anticipates that all transition matrix elements are only weakly dependent on energy. ω_{i} and ω_{s} are the frequency of the incident and the scattered light, and $\hbar\alpha$ is the width of the electronic states for which 0.01 eV was found to be appropriate. With these values the contributions from all tubes were again weighted with the same Gaussian line as used above and the result was summarized to yield the calculated line shape. This shape reproduces the experimental data very well in the following sense: (i) The fine structure in the Raman line is retained; (ii) it changes dramatically with the selected laser energy ω_{i}; and (iii) the calculated positions for maximum intensity change periodically with the laser energy. The peak intensities change periodically as well but quantitative comparison needs the evaluation of matrix elements.

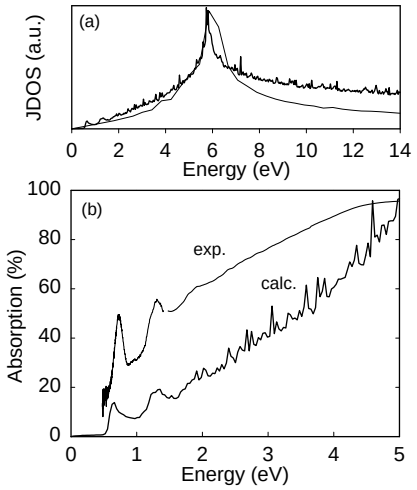

FIG. 3. Added joint density of states for all geometrically allowed nanotubes with radial breathing mode frequency between 145 and 220 cm^{-1} (noisy line) and joint density of states for the graphene sheet (dashed line) (a). Comparison between the added joint density of states (calc) and an absorption spectrum (exp) in the low energy range of the graphene band (b).

Considering the calculated results for excitation with all laser lines, the peak positions for the Raman response can be evaluated and thus allows a direct comparison with the experimental results from Fig. 2. The open circles and the dashed line are the calculated data. However, all calculated frequencies were uniformly up-shifted by 8.5%. The overall match between experiment and calculation is now very good and even the oscillations with the laser energy are rather well reproduced by the latter.

The requested up-shift is definitely beyond any error in the calculation and has thus an intrinsic origin. It is a consequence of the packing of the tubes into bundles. Since the calculations were performed for isolated tubes, the up-shift of about 8% is safely assigned to a strong intertube interaction due to van der Waals forces.

The main parameters entering the evaluation are the $pp\pi$ matrix element γ_0, the excited state lifetime $1/\alpha$, the width of the Lorentzian lines Γ_L, and the parameters for the Gaussian function. The latter are pretty well-defined for our samples from electron microscopy and x-ray analysis. Γ_L determines the fine structure for the calculated spectra and is as such independent of other parameters. γ_0 and α are crucial and not independent. They are very sensitive to peak position and peak height. A 5% change in γ_0 can lead to a 10 cm^{-1} shift in the peak position of the RBM mode in a particular spectrum. However, what counts is the average shift for all peak positions evaluated. In fact, from plots such as Fig. 2, a quantitative error in the form of a root mean square deviation of the experiment from the calculation can be defined as a function of the frequency scaling factor. We have varied both γ_0 and α in certain ranges and found a minimum error of 1.2% for the frequency scaling factor of 1.085. From the distribution function used for the fit only 4% of the tubes are (10,10).

Explicit examples for a calculated line pattern as compared to the experiments are depicted in Fig. 4. The good agreement between calculated and observed line shapes is evident, in particular for the higher energy excitation. Again, the agreement required an up-shift of the calculated spectra by 3%, 8%, and 13%, respectively, for the three spectra presented.

The remaining discrepancies in Figs. 2 and 4 are natural and due to the simplifications used in the model.

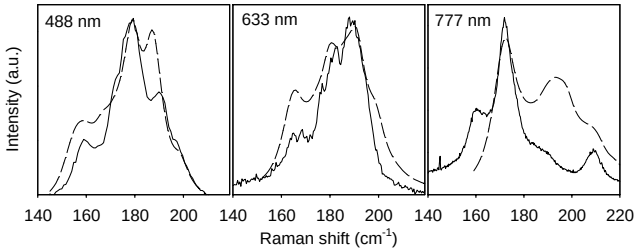

FIG. 4. Comparison between observed (−) and calculated (− −) pattern for the radial breathing mode for excitation with three different laser lines.

The periodicity in the resonance excitation is considered as a consequence of the periodicity in the Van Hove singularities.

A rather strong interaction for SWCNTs in a bundle was recently predicted theoretically [15] and also claimed from the observation of a large pressure coefficient for the RBM [16]. From a most recent calculation based on a molecular dynamical generalized tight binding model [17] and from a pair potential approach [18], a 7% and an 11% up-shift, respectively, of the RBM frequency due to the tube-tube interaction was found in excellent agreement with our results. Also, the optimum values obtained in this work for γ_0 and α are in very good agreement with results from Ref. [9].

In summary, the analysis for the Raman response of the RBM in SWCNTs demonstrates that in laser ablation grown material all geometrically allowed helicities are present. Since from the 80 tubes considered in the calculations only four are armchair and six are zigzag, the response from the chiral tubes dominates the spectra and in turn will dominate all experiments carried out on bulk SWCNT material. The observed results are straightforwardly extrapolated to SWCNTs prepared by other techniques.

This work was supported by the FFWF in Austria, Project No. P12924-tph, and by Grants No. OTKA T022980 and No. OTKA T030435 in Hungary. The supply of SWCNT from the Center for Nanoscale Science and Technology at Rice University and valuable discussions with G. Kresse are greatly acknowledged.

[1] A. Thess *et al.,* Science **273**, 483 (1996).
[2] J. M. Cowley, Chem. Phys. Lett. **97**, 379 (1997).
[3] J. W. Wildör *et al.,* Nature (London) **391**, 59 (1998).
[4] L. Henrard *et al.,* Synth. Met. **103**, 2533 (1999).
[5] H. Kuzmany *et al.,* Europhys. Lett. **44**, 518 (1998).
[6] E. Anglaret *et al.,* Carbon **36**, 1815 (1998).
[7] A. Rao *et al.,* Science **275**, 187 (1997).
[8] A. Kasuya *et al.,* Phys. Rev. Lett. **78**, 4434 (1997).
[9] M. A. Pimenta *et al.,* J. Mater. Res. **13**, 2396 (1998).
[10] S. Bandow *et al.,* Phys. Rev. Lett. **80**, 3779 (1998).
[11] J. B. Renucci, R. N. Tyte, and M. Cardona, Phys. Rev. B **11**, 3885 (1975).
[12] C. T. White and J. W. Mintmire, Nature (London) **394**, 29 (1998).
[13] J. Kürti *et al.,* Phys. Rev. B **58**, 8869 (1998).
[14] R. B. Martin and L. M. Falicov, Top. Appl. Phys. **8**, 79 (1975).
[15] Y.-K. Kwon *et al.,* Phys. Rev. B **58**, 13 314 (1998).
[16] U. D. Venkateswaran *et al.,* Phys. Rev. B **59**, 10 928 (1999).
[17] P. Eklund (private communication).
[18] L. Henrard Phys. Rev. B **60**, 8521 (1999).